

Super-resolution reconstruction of images based on uncontrollable microscanning and genetic algorithm*

DAI Shao-sheng (代少升), LIU Jin-song (刘劲松)**, XIANG Hai-yan (向海燕), DU Zhi-hui (杜智慧), and LIU Qin (刘琴)

Chongqing Key Laboratory of Signal and Information Processing, Chongqing University of Posts and Telecommunications, Chongqing 400065, China

(Received 22 April 2014)

©Tianjin University of Technology and Springer-Verlag Berlin Heidelberg 2014

Aiming at these disadvantages like lack of details, poor contrast and blurry edges of infrared images reconstructed by traditional controllable microscanning super-resolution reconstruction (SRR), this paper proposes a novel algorithm, which samples multiple low-resolution images (LRIs) by uncontrollable microscanning, and then uses LRIs as chromosomes of genetic algorithm (GA). After several generations of evolution, optimal LRIs are got to reconstruct the high-resolution image (HRI). The experimental results show that the average gradient of the image reconstructed by the proposed algorithm is increased to 1.5 times of that of the traditional SRR algorithm, and the amounts of information, the contrast and the visual effect of the reconstructed image are improved.

Document code: A **Article ID:** 1673-1905(2014)04-0313-4

DOI 10.1007/s11801-014-4067-x

For the limitation of material and technology, the density of complementary metal-oxide-semiconductor (CMOS) transistor photosensitive element in existing infrared focal plane arrays (IRFPAs) can not satisfy the demand for acquiring high-resolution infrared images. While microscanning imaging technology may get several similar low-resolution images (LRIs) of the same scene with the IRFPAs, and then the high-resolution images (HRIs) can be reconstructed using these LRIs. Now the common realization methods of microscanning, like mechanical translation, scanning mirror and slab rotation, obtain steerable displacements between optical system and detector to achieve controllable microscanning imaging. In practical application, the weather, location, human and material resources will affect the microscanning inevitably, thus not all imaging processes are controllable accurately. But as long as there are non-integral displacements between LRIs, they can be used to reconstruct HRI. Genetic algorithm (GA) is an optimization-seeking algorithm based on natural selection and genetic mechanism. It has been applied to artificial intelligence, life science and image reconstruction fields for its powerful ability to acquire the optimum solution adaptively. This paper innovatively uses LRIs as chromosomes, and the desired HRI is obtained by super-resolution reconstruction^[1-8] based on LRIs of final generation from multiple evolutions.

Now available working modes of controllable microscanning, including 2-step, 4-step, 9-step and 16-step, are

shown in Fig.1. Take 4-step mode as an example. The detectors gather and save the first LRI in location0, and then move to location1, location2 and location3 successively to acquire and store the remaining 3 images. Different steps determine various sequences, directions and periods of detector movements. The more scanning steps, the more LRIs obtained, and the higher the reconstructed image resolution is.

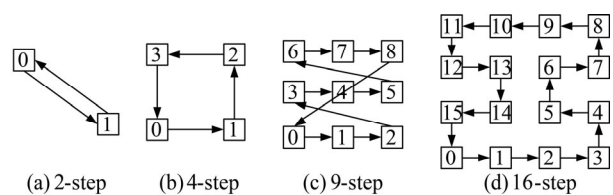


Fig.1 Four working modes of controllable microscanning

In practical application, for the influences from nature, like mountains, cliffs, rainstorms and limitations of human and material resources, not all microscanning imaging processes are controllable accurately. However, initial HRI can be reconstructed if there are non-integral displacements between acquired LRIs. Now IRFPAs based on uncontrollable microscanning are usually installed at steamships, vehicles, planes or other movable platforms, and detectors will shake uncontrollably following the

* This work has been supported by the National Natural Science Foundation of China (No.61275099), and the Project of Key Laboratory of Signal and Information Processing of Chongqing (No.CSTC2009CA2003).

** E-mail: liujinsong1991@yeah.net

movements of installation platforms to get LRIs.

When simulating the uncontrollable microscanning, in order to reduce the complexity of the subsequent GA operation, we regulate that the detectors can only move to four directions of up, down, left and right with the maximum displacement of one pixel distance, explained as

$$f_{k+1}(i, j) = f_k(i \pm \Delta i, j \pm \Delta j), \quad (1)$$

where f represents LRI, and Δi and Δj refer to the horizontal displacement and vertical displacement respectively between the k th and the $(k+1)$ th low-resolution frames, which are restrained by

$$\Delta i \cdot \Delta j = 0, \max(\Delta i) = 1, \max(\Delta j) = 1. \quad (2)$$

Although the shifts obey the Poisson distribution as a whole, the direction and the specific displacement of detector movements are all random and uncontrollable. For avoiding the extreme phenomenon that there is no frame gathered in a certain direction, increasing the number of obtained LRIs is necessary.

In GA^[9], the solution space called genetic space includes every possible solution demonstrated in the shape of matrices. These matrices and elements in the matrices are called chromosomes and genes, respectively. First the algorithm produces several new chromosomes based on original chromosomes to constitute the initial population in a certain method, and then utilizes proper fitness function to evaluate each chromosome. According to fitness values, the corresponding chromosomes can be processed with genetic operations, including selection, cross and variation. Finally, the chromosome with the worst fitness will be eliminated, while the chromosome with the best fitness will be inherited to the next generation. After several generations, the final generation will get the optimal chromosomes and genes, in which the individual with the best fitness is the optimal solution we need.

When it comes to digital image processing (DIP), the images are the so-called chromosomes, and the information in the image, like gray levels, colors or brightness of pixels, is the genes of the corresponding chromosome. All the chromosomes constitute a genetic space.

The paper uses real-value coding to encode images. If the size of LRIs is $M \times N$, the gray values of the $M \times N$ pixels are genes of corresponding two-dimensional chromosomes, and the values of genes are from 0 to 255.

To avoid the influence from interpolation on gathered LRIs in GA, the paper innovatively uses LRIs as genetic units and references to constitute the initial population. For any LR frame $f_k \in M \times N$, the formula describing how to creating the initial population can be expressed as

$$\mathbf{I} = P(\mathbf{f} + \sigma \boldsymbol{\beta}), \quad (3)$$

where \mathbf{f} is the pixel gray value of f_k in the form of vector, σ is a range parameter defined as 1 in this paper, $\boldsymbol{\beta}$ represents a number vector with its elements distributed evenly from -1 to $+1$, \mathbf{I} refers to the new generated low-resolution frame in the shape of vector, and P is an operator to limit

the vector element value from 0 to 255, which is defined as

$$P(x) = \begin{cases} 0, & x \leq 0 \\ 255, & x \geq 255 \\ x, & \text{else} \end{cases} \quad (4)$$

On the basis of each initial LRI, the initial population including plenty LRIs will be generated by several such operations according to Eqs.(3) and (4).

Super-resolution reconstruction (SRR) is a typical ill-posed and inverse problem, so we introduce the regularization term^[10] to resolve SRR problem. Based on the reason, the fitness function in this paper is formed by traditional fitness function and an additional regularization term. The new fitness function is described as

$$E(\mathbf{I}) = \|\mathbf{I} - \mathbf{H}\mathbf{L}\| + \lambda \|\mathbf{C}\mathbf{L}\|, \quad (5)$$

where $E(\mathbf{I})$ represents the fitness value of the chromosome composed of LRI \mathbf{I} , $\|\mathbf{I} - \mathbf{H}\mathbf{L}\|$ refers to the deviation between the real HRI and the estimated HRI, $\lambda \|\mathbf{C}\mathbf{L}\|$ is the so-called regularization term to improve ill-posed condition of the inverse problem, \mathbf{H} is the degradation matrix between HRI and LRI, which describes the degradation processes like blurring, movement, down-sampling and noise jamming, \mathbf{L} is the HRI produced by interpolation from the corresponding LRI, λ is the regular parameter to adjust the proportion between $\|\mathbf{I} - \mathbf{H}\mathbf{L}\|$ and $\lambda \|\mathbf{C}\mathbf{L}\|$, and \mathbf{C} refers to a high-pass filter like Gaussian filter or Laplace filter.

From the analysis of fitness function, the smaller fitness function value is, the smaller error between the real HRI and the estimated HRI. That is to say, the more accurate the LRI providing information is, the better the reconstruction result is. Thus the LRI with the minimum fitness function value is the best chromosome.

Selection operation refers to a process of selecting chromosomes with better performance and inheriting them to the next generation. This paper uses the principle of protecting the optimal chromosome. That is, compute the fitness value of each chromosome, and the optimal chromosome which has the minimum fitness value in current generation does not experience the genetic operations including cross and variation. The other chromosomes will be processed by the following cross operation and variation operation. Finally, the chromosome with the worst fitness is replaced by the optimal one.

Cross operation is a process of pairing chromosomes randomly and exchanging their part genes with a certain probability. In DIP field, cross operation is operated by exchanging part pixels of coupled images, including point-exchange, row-exchange (or column-change) and block-exchange demonstrated in Fig.2. Take point-exchange as an example. As shown in Fig.2(a), the images a(1) and a(2) are a couple of pictures to be crossed, and the triangular pixel point of a(1) and the pentagonal pixel point of a(2) are the corresponding points to be exchanged. After cross operation, we can find that the triangular point in a(1) is replaced with the pentagonal one of a(2), and the pen-

tagonal point in a(2) is exchanged by the triangular one of a(1), while other pixel points in both images are not changed, which are illustrated as a(3) and a(4). Like point-exchange, row(column)-exchange and block-exchange are the similar processes, and the only difference is that the pixels to be exchanged in a couple of images are not separate points, but a whole pixel row(column) or a pixel block. As the features of an image are reflected by its block average value and variance generally, we adopt block-exchange to implement the cross operation.

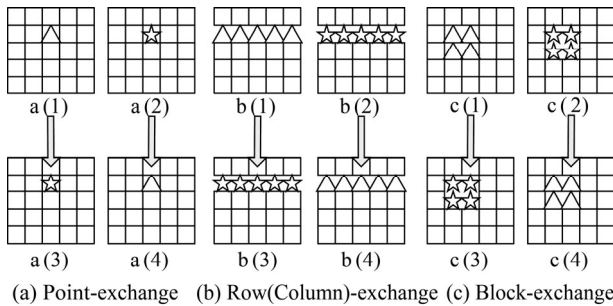


Fig.2 Three common exchange modes of cross operation

Variation operation is a process to change a certain gene or some genes of a certain chromosome in the population. In DIP field, variation operation is operated by changing part pixels of the current image. There are three main variation patterns, including point-variation, row(column)-variation and block-variation, whose difference is that the changed image region is a pixel point, a whole pixel row(column) or a pixel block. Similar to cross operation, point-variation does not make sense for images, thus this paper adopts block-variation to change the pixels of images. Because the process is equivalent to the addition of random noise to the original LRI chromosomes in the step of generating the initial population, to reduce the influence of the so-called noise in GA, we adopt the average operation as the variation process. That is, use the average gray value of the current block to replace the gray value of the center pixel in the block. Compared with traditional variation process, the new variation operation not only reduces the noise jamming, but also avoids the premature convergence in conventional GAs to some extent.

In the simulation of uncontrollable microscanning, we regulate that the detectors centered on the current position can only move to four directions of up, down, left and right with the maximum displacements of one pixel. 100 frames of LRI are acquired in this way, and the whole procedure can simulate degradation factors like dimming, moving and down-sampling in real imaging process. Generate the initial population based on each original LRI, and then process chromosomes with genetic operations including selection, cross and variation according to corresponding fitness values to eliminate the chromosomes with the worst fitness and inherit those with the best fitness to the next generation. The genetic process is repeated until reaching the specified number of genetic iterations. The final generation will get the optimal chromosomes, which are optimal LRIs virtually, and the needed HRI can be reconstructed from these best LRIs by regularized SRR.

To illustrate the effectiveness of GA, the relationship between the generation and the fitness function value is described in Fig.3. In Fig.3, the fitness function value is an average level of a certain generation, which declines with the increase of generation. Furthermore, after about 120 generations of evolution, the evolution is saturated with the minimum fitness function value, and the optimal LRIs will be obtained. Then we can use the best LRIs to reconstruct the desired HRI.

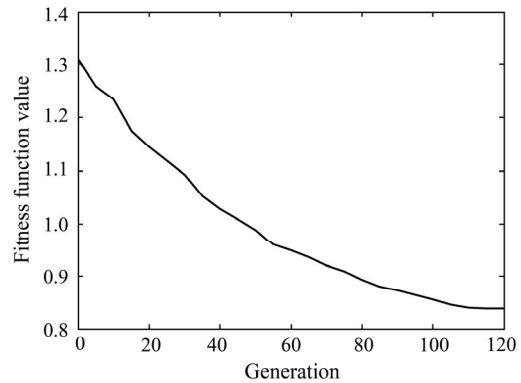


Fig.3 The relationship between generation and fitness value

The reconstructed images by different SRR algorithms are demonstrated in Fig.4. In Fig.4(c) and Fig.4(e), the average fitness values of these LRIs are about 1.3 and 0.85 which are shown in Fig.3.

From visual effect, the algorithm proposed by this paper reconstructs the HRI perfectly. In Fig.4(f), the outlines of man and car are distinct to observe. Fig.4(b) reconstructed by interpolation SRR and Fig.4(d) reconstructed by traditional regularized SRR without GA can not reveal the edges of the car and the man clearly. To avoid the subjectivity and one-sidedness gained by visual effect, we apply certain objective evaluation standards including information entropy, average gradient^[11] and contrast^[12] to measure the reconstruction effect. The results are illustrated in Tab.1.





Fig.4 (a) A gathered LRI; (b) The image reconstructed by bicubic interpolation; (c) The set including the LRIs of the first generation; (d) The image reconstructed by LRIs from (c) using traditional regularized SRR; (e) The set including the optimal LRIs of the final generation; (f) The image processed by the proposed algorithm, which is reconstructed by the optimal LRIs from (e)

Tab.1 Objective evaluation standards of the reconstructed images

| | Information entropy | Average gradient | Contrast |
|----------|---------------------|------------------|----------|
| Fig.4(b) | 6.670 3 | 0.021 6 | 20.674 0 |
| Fig.4(d) | 6.727 9 | 0.032 0 | 21.192 3 |
| Fig.4(f) | 6.733 5 | 0.033 3 | 21.284 2 |

From Tab.1, the amounts of information, average gradient and contrast of the image reconstructed by the new algorithm are all improved, especially the average gradient in Fig.4(f) is increased to 1.5 times of that of the traditional SRR algorithm. As a whole, the new algorithm we propose not only accomplishes SRR, but also realizes image enhancement and restoration to some extent as well.

To avoid the disadvantages like lack of details, poor contrast and blurry edges of infrared images reconstructed by traditional controllable microscanning SRR, this paper proposes a novel algorithm. The new algorithm samples multiple LRIs by uncontrollable microscanning, and then

uses LRIs as chromosomes of GA. After several generations of evolution, optimal LRIs are obtained to reconstruct the HRI. The experimental results show that the amounts of information, definition and visual effect of the image reconstructed by the new algorithm have great improvements. In summary, the proposed algorithm not only accomplishes SRR, but also realizes image enhancement and restoration to some extent as well.

References

- [1] ZHU Bo, LI Hua, GAO Wei and SONG Zong-xi, Journal of Optoelectronics·Laser **24**, 2024 (2013). (in Chinese)
- [2] Tsai R. Y. and Huang T. S., Advances in Computer Vision and Image Processing **1**, 317 (1984).
- [3] Hardie R. C. and Barnard K. J., Optics Express **20**, 21053 (2012).
- [4] ZHANG Cheng, YANG Hai-rong, CHENG Hong and WEI Sui, Journal of Optoelectronics·Laser **24**, 805 (2013). (in Chinese)
- [5] Park S. C., Park M. K. and Kang M. G., IEEE Signal Processing **20**, 21 (2003).
- [6] Elad M and Hel-Or Y, IEEE Transactions on Image Processing **10**, 1187 (2001).
- [7] Farsiu S., Robinson M. D., Elad M. and Milanfar P., IEEE Transactions on Image Processing **13**, 1327 (2004).
- [8] Schultz R. R., Meng L. and Stevenson R. L., Journal of Visual Communication and Image Representation **9**, 38 (1998).
- [9] Ye F., Su L. and Li S., Chinese Optics Letters **4**, 386 (2006).
- [10] Haiyong Liao, Fang Li and Michael K. Ng, Journal of Optical Society of America A **26**, 2311 (2009).
- [11] Yang J., Wright J. and Huang T. S., IEEE Transactions on Image Processing **19**, 2861 (2010).
- [12] DAI Shao-sheng and LIU Yong-peng, Semiconductor Optoelectronics **33**, 891 (2012). (in Chinese)